TiS Trends in Sciences
TRENDS IN SCIENCES 2027; 24(1): 13821
SPRINT Scholarly Publishing and Repository Integration Center
https://doi.org/10.48048/tis.2027.13821
RESEARCH ARTICLE

Synergistic Biopolymer Films from Sago Starch/Poly (Vinyl Alcohol) Blends: Structure-property Relationships

Pattamarat Rattanachuay[1], Sameela Cheming[1], Lapporn Vayachuta[2] and Jareerat Ruamcharoen[1,*]

[1]Department of Science, Faculty of Science and Technology, Prince of Songkla University, Pattani 94000, Thailand
[2]National Nanotechnology Center (NANOTEC), National Science and Technology Development Agency (NSTDA), Pathum Thani 12120, Thailand

([*]Corresponding author's e-mail: jareerat.su@psu.ac.th)

Received: 14 March 2026, Revised: 18 June 2026, Accepted: 18 June 2026, Published: 15 August 2026

Abstract

In this study, sago starch (SS) was blended with polyvinyl alcohol (PVA) at SS/PVA ratios of 90/10, 80/20, 70/30, 60/40, 50/50, and 40/60 to improve the physical, mechanical, and structural properties of starch-based films. The effect of PVA incorporation on film performance was systematically investigated. The results showed that moisture content do not significant decrease, while water solubility increased with increasing PVA content. Water vapor transmission values decreased with increasing PVA incorporation, indicating enhanced water vapor barrier properties of the blended films. The SS/PVA (70/30) film exhibited the lowest WVTR (0.00073 $g.cm^{-2}.h^{-1}$), suggesting optimal intermolecular hydrogen bonding and compact network formation, while higher PVA content slightly increased WVTR due to increased free volume and partial disruption of the polymer network. Water contact angle analysis showed that the incorporation of PVA decreased the surface hydrophilicity of SS/PVA blend films, with contact angle values decreasing from 89.3° for neat SS film to 43.8° for neat PVA film. The SS/PVA blends exhibited contact angle (50° - 70°), indicating that intermolecular hydrogen bonding between SS and PVA influenced surface wettability. Tensile strength increased with increasing PVA content, while the modulus gradually decreased, indicating reduced stiffness and enhanced flexibility of the films. In addition, elongation at break significantly increased at higher PVA ratio, confirming improved ductility and flexibility of the SS/PVA blend films. FTIR analysis confirmed hydrogen-bonding interactions between SS and PVA hydroxyl groups, which contributed to the improved film properties. XRD and DSC analyses revealed that the blend films exhibited a semi-crystalline structure, with crystallinity increasing as the PVA content increased. SEM observation further showed that films containing higher PVA ratio (SS50/PVA50 and SS40/PVA60) exhibited rougher and more heterogeneous surface morphologies.

Keywords: Biopolymer film, Sago starch, Poly (Vinyl alcohol), Water vapor transmission, Water contact angle, UV-visible absorbance, Tensile property

Introduction

Starch-based biopolymer films have attracted significant attention as sustainable alternatives to conventional plastics due to their biodegradability, abundance, and renewable origin. They are typically produced from starch and plasticizers, with optional additives to enhance functional properties [1,2]. Starch, composed of amylose and amylopectin, is readily biodegradable, making film more environmentally friendly than persistent synthetic plastic. Various starch sources, such as corn, potato, and cassava, can be used depending on availability and desired properties [3,4]. However, starch-based films are inherently rigid and brittle due to strong intermolecular interactions, resulting in low flexibility. Their high hydrophilicity,

arising from abundant hydroxyl groups, leads to significant water absorption, high solubility, and elevated water vapor permeability, limiting their application in food packaging. To address these limitations, plasticizers such as glycerol and sorbitol are commonly added to improve flexibility and processability, although this may reduce mechanical strength [4-6]. Chemical modifications, including cross-linking and esterification, are also used to enhance film properties [7,8]. Despite these challenges, starch-based films show strong potential in food packaging, agriculture, and biomedical applications due to their biodegradability and biocompatibility [9-12].

Sago starch has emerged as a promising feedstock for biopolymer film development due to its abundance in Southeast Asia, particularly Southern Thailand, and its complete biodegradability. Derived from the trunk of *Metroxylon* sagu (Arecaceae), it is characterized by high carbohydrate content and broad applicability in food and non-food sectors [13,14]. The crop is highly productive, yielding more than 4 tons of starch per acre, which is considerably higher than that of rice. The extracted starch is commonly processed through rasping, washing, filtration, sedimentation, drying, and milling prior to further utilization. Sago starch granules are generally oval-shaped, with sizes ranging from 20 - 40 μm, and contain high starch content of approximately 82.7% in the stem and up to 88.6% after purification [15-17]. Its amylose content in the range of 24% - 30% should be good for film-forming ability and provides acceptable mechanical properties. However, conventional sago starch films still have limitations due to their high hydrophilicity and brittleness, which reduce material stability and durability. In addition, sago starch exhibits low swelling capacity, limited water solubility, and a high tendency for retrogradation, which may negatively affect film properties during storage and long-term use [18].

Polyvinyl alcohol (PVA) is a water-soluble synthetic polymer known for its excellent film-forming ability, adhesion, flexibility, biodegradability, and non-toxic nature [19-22]. Its properties are influenced by the degree of hydrolysis and processing condition. Owing to these properties, PVA has been extensively investigated for food packaging application, particularly as edible coating for fruit and vegetable to extend shelf life and reduce postharvest deterioration [22]. In addition, PVA can function as a barrier coating to improve moisture and oxygen resistance, thereby enhancing food preservation and product quality. The properties of PVA film can be tailored through various modification approaches. The incorporation of plasticizers improves flexibility and toughness, while cross-linking enhances mechanical properties and water resistance [21,22]. Furthermore, blending PVA with other polymers or functional additives enables further optimization of its physicochemical and mechanical properties [20-22].

Starch-based films generally exhibit poor mechanical strength and high moisture sensitivity, which limit their practical applicability. To overcome these limitations, starch is commonly blended with polyvinyl alcohol (PVA). This blending strategy has been shown to significantly improve mechanical performance, water resistance, and thermal stability, primarily due to enhanced intermolecular interactions and the formation of a more cohesive and homogeneous polymer network [22-24]. However, starch is inherently susceptible to retrogradation and recrystallization process that leads to undesirable changes in material properties, such as increased rigidity, brittleness, and reduced shelf-life stability. Although starch/PVA blends have been widely studied, the use of sago starch (SS) remains relatively limited compared with cassava, corn, and potato starch [25-29]. Furthermore, differences in molecular structure, crystallinity, and chain mobility between SS and PVA may influence blend compatibility and film performance. The predominantly amorphous structure of gelatinized SS and the semicrystalline nature of PVA can lead to phase heterogeneity, uneven molecular distribution, and variations in water affinity, transparency, and structural stability. Consequently, the influence of SS/PVA blend ratio on the structure-property relationships of biodegradable films remains insufficiently understood. Therefore, this study systematically investigates a broad range of SS/PVA blending ratios and correlates their mechanical, thermal, barrier, surface, and structural properties to provide a deeper understanding of sago starch-based biodegradable films.

In this study, sago starch was extracted from sago palm and characterized in terms of its chemical composition, molecular structure, and morphology. The effect of blending sago starch with PVA on the physical and mechanical properties were systematically

investigated. Additionally, molecular interaction between sago starch and PVA was analyzed by using Fourier transform infrared spectroscopy (FTIR) and X-ray diffraction (XRD). The morphology and structural homogeneity of the SS/PVA films were further examined using scanning electron microscopy (SEM) to establish correlation between microstructure and macroscopic properties of the blended films.

Materials and methods

Materials

Sago palms (*Metroxylon* sagu Rottb.) was provided from Paka Harang Subdistrict, Mueang Pattani District, Pattani, Thailand. Glycerol, analytical reagent grade with 99.5% purity, was obtained from Ajax Finechem Pty Ltd. (Australia). Polyvinyl alcohol (PVA) powder (MW = 70,000 $g.mol^{-1}$, degree of hydrolysis 87% - 90%) was obtained from Sigma-Aldrich Limited.

Sago starch extraction method

Sago starch extraction was initiated by stripping the outer bark from the palm trunk to isolate the starchy pith. The pith was subsequently disintegrated using a modified mechanical grater designed to minimize sample contamination. The resulting material was mixed with water and filtered through a fine cloth to separate the fibrous residue; the starch milk was then allowed to undergo sedimentation for 8 h. Following decantation of the supernatant, the starch was dewatered by wrapping and draining for 5 days, yielding fresh starch with a moisture content of 64.7% - 73.3%. The product was then sun-dried, milled, and passed through a 149-mesh sieve. For the production of sago pearls, partially moist starch was granulated and subjected to further drying. The proximate and chemical compositions, including amylose, amylopectin, moisture, protein, fat, ash, and dietary fiber, were determined according to AOAC (1995) standard method [30]. The chemical and crystalline structures of the sago starch granules were characterized using Fourier transform infrared (FTIR) spectroscopy and X-ray diffraction (XRD) techniques, respectively. Granule morphology was examined via scanning electron microscopy (SEM).

Preparation of SS/PVA Blend

Sago starch (SS) was blended with polyvinyl alcohol (PVA) using a microwave-assisted solution casting method. Initially, 5 g of SS and glycerol (30 wt% of starch) were dispersed in distilled water, and the suspension was heated in a microwave oven at 300 W for 90 s to induce starch gelatinization. Subsequently, PVA was added to the gelatinized starch solution and further heated for 30 s to obtain a homogeneous gel. The resulting mixture was cast into polyethylene mold and dried in an oven at 50 °C for 24 h to allow solvent evaporation. After drying, the SS/PVA films were carefully peeled from the molds and stored in a dehumidifier prior to characterization. The prepared biofilms were produced with different SS/PVA weight ratios of 100/0, 90/10, 80/20, 70/30, 60/40, 50/50, 40/60 and 0/100, respectively.

Biopolymer film characterization

Moisture content determination

The moisture content of the samples was determined according to the AOAC (2000) standard method [30]. Film samples were cut into pieces measuring 2×2 cm, weighed accurately, and placed in drying containers. The samples were then dried in a hot-air oven at 110 °C for 1 h, or until a constant weight was achieved. After drying, the samples were cooled in a desiccator and reweighed. The moisture content (MS) was calculated based on weight loss before and after drying as shown in Eq. (1);

$$\text{MS}\ (\%) = \frac{W_i - W_f}{W_i} \times 100 \quad (1)$$

where W_i is initial weight of the sample before drying (g) and W_f is final weight of the sample after drying (g)

Water solubility determination

The SS/PVA film samples were cut into pieces measuring 2×2 cm and accurately weighed. The samples were then immersed in distilled water at room temperature for a predetermined period. After immersion, the film samples were filtered to separate the water-soluble fraction from the insoluble residue. The remaining insoluble portion was collected and dried in a hot-air oven at 100 °C until a constant weight was

obtained. The water solubility (WS) of the SS/PVA biopolymer films was calculated according to Eq. (2);

$$WS\ (\%) = \frac{W_i - W_f}{W_i} \times 100 \quad (2)$$

Where W_i is initial weight of the sample before immersion in distilled water (g) and W_f is final weight of the sample remaining insoluble portion.

Water vapor transmission test

The water vapor transmission test was conducted according to the ASTM E96 standard method (ASTM E96-00, 2000) as modified by Ruamcharoen *et al*. [31,32]. Prior to testing, the films were conditioned by heating at 50 °C for 2 h. Circular specimens, cut to match the diameter of container, were weighed and their thickness measured. Each bottle was filled with silica gel, weighed, and then sealed with the film samples before being placed in a desiccator maintained at 75% relative humidity (RH). The weight of the bottles was recorded at 6, 24, 48 and 72 h. The water vapor transmission was calculated according to Eq. (3);

$$WVTR = \frac{W_t - W_i}{\Delta t \times A} \quad (3)$$

where W_i is initial weight of film, W_t is weight of the water vapor absorbed sample, t is time duration and A is area of film.

Contact angle measurement

The water contact angle of the SS/PVA films was measured by first preparing clean, smooth specimens and placing them on a flat, stationary surface. Furthermore, the contact angles were determined using a Dataphysics Model TC/TPC 150 contact angle instrument via the sessile drop method. A 5 µL droplet of distilled water was deposited onto each film. Images of the droplets were captured, and the contact angle (θ) was determined using SCA 20 analysis software. The measured angles provide an indication of the surface hydrophilicity or hydrophobicity. All measurements were performed in five replicates.

Mechanical test of SS/PVA biopolymer films

The mechanical properties of the SS/PVA films were determined using a universal tensile testing machine at room temperature. Tensile test was performed at a crosshead speed of 30 mm·min^{-1} with an initial grip separation of 30 mm, in accordance with ASTM D882-12 [33]. Rectangular specimens (10×100 mm) were conditioned at room temperature for 48 h prior to testing. Tensile strength (TS) and elongation at break (%EB) were calculated. At least five replicates were tested, and only data from specimens that were fractured at the film center were considered.

UV-Visible absorbance of SS/PVA biopolymer films

The UV-visible absorbance of the SS/PVA films was evaluated following the method described by Awang Wahab *et al*. [34]. Rectangular film specimens (1×2 cm) were analyzed over a wavelength range of 200 - 400 nm using a UV-visible spectrophotometer (Lambda 35, PerkinElmer, USA). For each specimen, the light absorption values were recorded in triplicate.

Fourier transform infrared spectroscopy analysis

The chemical structure of the SS/PVA films was analyzed using an FTIR spectrometer (Bruker Tensor 27, Germany). The biopolymer films were directly mounted on the FTIR sample holder, and spectra were recorded over the wavenumber range of 400 - 4,000 cm^{-1} with a resolution based on 32 accumulated scans. The spectra were analyzed for band shifts, intensity changes, and the appearance or disappearance of characteristic peaks to evaluate hydrogen bonding, molecular compatibility, and structural changes within the films, providing insight into the interactions between sago starch and PVA.

X-Ray diffraction analysis

X-ray diffraction (XRD) analysis was conducted using a Philips X'Pert MPD (Netherlands) instrument to characterize the crystalline structure of the SS/PVA films. Film specimens were cut into appropriate dimensions and mounted on the sample holder to ensure a flat and uniform surface. Measurements were performed using Cu-Kα radiation (λ = 1.5406 Å) at an operating voltage of 40 kV and a current of 40 mA.

Diffraction patterns were recorded over a 2θ range of 5° - 50°, with a step size of 0.02° and a scanning rate of 2°/min. The degree of crystallinity (X_c) was calculated from the XRD patterns using the ratio of the crystalline peak area to the total area, as expressed by the following equation.

$$X_c(\%) = \frac{A_c}{A_c + A_a} \times 100 \quad (4)$$

where A_c is the area of the crystalline peaks and A_a is the area of the amorphous region.

Differential scanning calorimetry analysis

The melting behavior of the blends were determined by using Thermal Analysis System DSC 3+ Stare System (Mettler Toledo, Switzerland). Heating and cooling for both first and second cycles were done in a nitrogen atmosphere at the rate of 20 °C.min^{-1} from a temperature of 30 to 250 °C. The calibration in DSC was done by measuring the temperature and the enthalpy of indium melting.

Scanning electron microscopy analysis

The surface and cross-sectional morphology of composited films were examined using a scanning electron microscope (S3400N, Hitachi, Japan). For cross section analysis, the film was prepared by using the conventional liquid nitrogen cryogenic fracture method. Then, residual moisture in films was removed by vacuum at 25 °C for 18 h. The samples were coated with a thin layer of gold using a sputtering technique before analysis. SEM observations were carried out at an accelerating voltage of 15 kV. SEM micrographs were used to assess the dispersion of components, the presence of voids or cracks, and the overall structural integrity of the biopolymer films.

Results and discussion

Sago starch characterization

The extracted sago starch appeared as a fine, pale-pink powder with no visible impurities, indicating a high degree of purity and suitability for subsequent film preparation and other potential applications. The chemical composition of the extracted sago starch is presented in **Table 1**.

Table 1 Chemical composition of sago starch.

Chemical composition	Amylose	Protein	Fat	Ash	Moisture	Lignin	Fiber
Content (%)	23.84 ± 0.32	0.19 ± 0.01	0.04 ± 0.001	0.32 ± 0.00	13.95 ± 0.07	0.13 ± 0.00	0.54 ± 0.03

The amylose content of sago starch was 23.84 ± 0.32% comparable to tapioca starch and slightly lower than that of corn and rice starches [14,15]. This level is comparable to corn starch (approximately 28%) and is considered significantly higher than potato starch, though variations occur depending on the botanical source. The protein (0.19%) and fat (0.04%) contents were very low, indicating high starch purity. The moisture content (13.95%) was within the acceptable commercial range, ensuring storage stability and limiting microbial growth. Additionally, the low fiber content suggests minimal interference from cell wall component, contributing to improved digestibility, efficient gelatinization, and better processability.

SEM images (**Figure 1(a)**) showed that sago starch granules were discrete, mostly oval particles with smooth, intact surfaces and no visible cracks, indicating minimal structural damage during extraction. The granule size was relatively uniform, ranging from 20 - 40 μm, with slight variations likely due to differences in amylose-amylopectin organization. This is similar to the granule characteristics of sago starch as previously reported [15-17]. The XRD pattern (**Figure 1(b)**) revealed a mixed A type and B type crystalline structure, with characteristic peaks at 15.2° and doublets at 15.2°, 17.1°, 18.0°, and 23.2°, consistent with previous reports [15,17]. The FTIR spectrum of sago starch (**Figure 1(c)**) exhibits typical starch features, including a broad O-H stretching band (3,520 - 3,217 cm^{-1}) indicating hydrogen bonding, C-H stretching (2,920 - 2,930 cm^{-1}), and a band at 1,643 cm^{-1} associated with absorbed water. The characteristic peaks at 1,459 and 1,350 cm^{-1} corresponded to CH_2 and CH_3 bending modes, while the 980 - 1,060 cm^{-1} region reflected polysaccharide C-O-C

vibrations. The bands at 987 and 1,020 cm^{-1} represent crystalline and amorphous regions, respectively, confirming the presence of amylose and amylopectin [15].

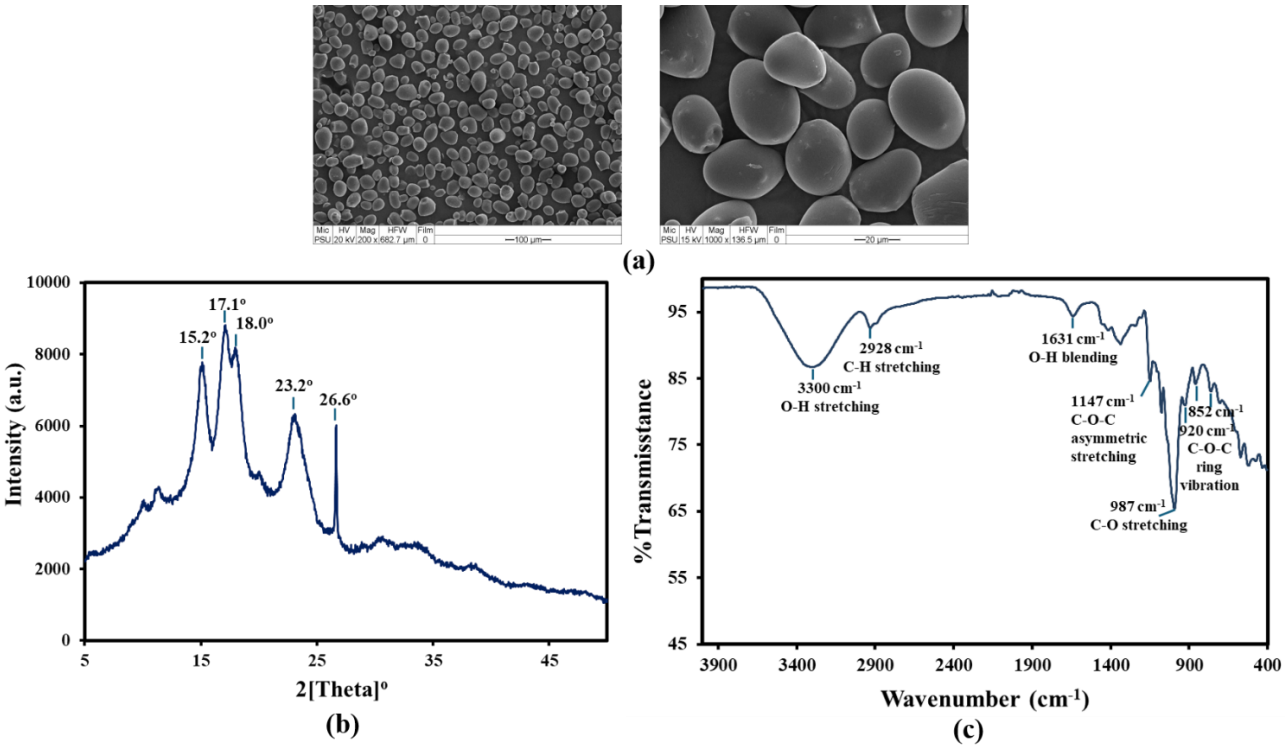


Figure 1 SEM micrographs (a), XRD pattern (b), and FTIR spectrum (c) of sago starch.

Characterization of water resistance properties of SS/PVA biopolymer films

Moisture content

Figure 2 presents the moisture content of SS, SS/PVA, and PVA films. The neat SS film exhibited a moisture content of 11.31%, which can be attributed to the hydrophilic nature of starch and the abundance of hydroxyl groups capable of forming hydrogen bonds with water molecules. Previous studies have shown that the moisture content of starch-based films varies considerably depending on the starch source and processing conditions, typically ranging from approximately 9% to 22% [35,36]. Upon incorporation of PVA at ratios of SS90/PVA10 and SS80/PVA20, the moisture content increased to 12.54% and 12.42%, respectively. At these ratios, the polymer network is likely less compact, with increased free volume and incomplete intermolecular interactions, allowing greater retention of water molecules. As the PVA content increases further (70/30 to 50/50), the moisture content slightly decreases. This reduction indicates improved intermolecular interactions and stronger hydrogen bonding between starch and PVA chains, resulting in a more compact network structure [27]. However, at higher PVA content (40/60), the moisture content slightly increased. This behavior may be associated phase separation or structural heterogeneity at higher PVA ratio could create localized domains that facilitate moisture retention.

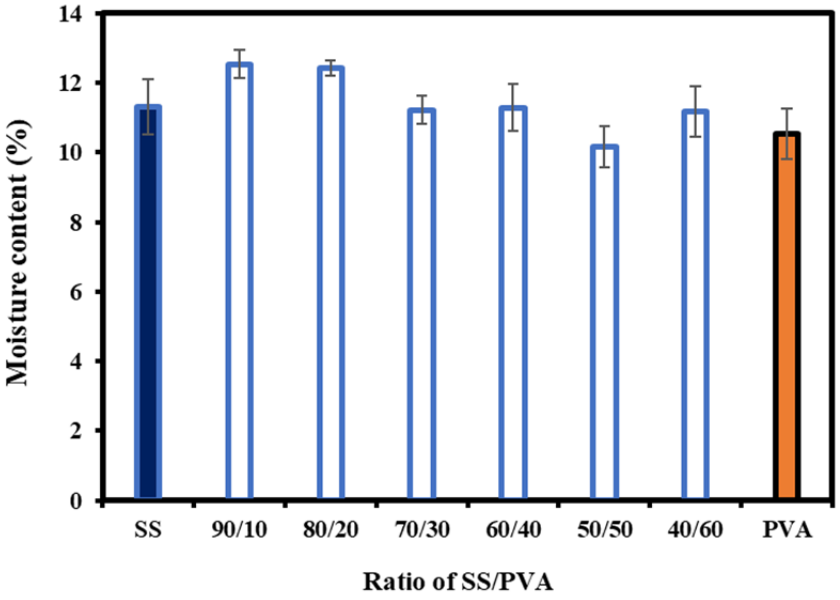


Figure 2 Moisture content of SS, PVA, and SS/PVA biopolymer films with varying blending ratios.

Water vapor transmission

The water vapor transmission (WVT) of starch (SS), PVA, and their blended films is shown in **Figure 3**. For all formulations, WVT decreased progressively with exposure time (6 - 72 h), indicating time dependent stabilization of water vapor diffusion through the film matrix. At 6 h, the SS film exhibited the highest WVTR (0.00153 $g.cm^{-2}.h^{-1}$), which is consistent with its hydrophilic nature and relatively loose polymer network. Incorporation of PVA reduced WVT due to its semi crystalline structure and its ability to form intermolecular hydrogen bonds with starch, thereby limiting diffusion pathways. The lowest WVTR was observed at the 70/30 ratio (0.00073 $g.cm^{-2}.h^{-1}$), suggesting optimal intermolecular interaction and network formation. However, further increasing PVA content (60/40 - 40/60) led to a slightly increase in WVT, likely associated with increased free volume and partial disruption of the hydrogen-bonded network. As time progressed (48 - 72 h), the insignificant differences between the formulations decreased, approaching a narrower WVTR range (0.00049 - 0.00053 $g.cm^{-2}.h^{-1}$), indicating that diffusion equilibrium had been reached. Notably, the reduction in WVT was not strictly proportional to PVA content, reflecting the complex interplay between polymer miscibility, phase distribution, and free volume within the matrix. The SS50/PVA50 film exhibited improved intermolecular interactions and enhanced chain packing, resulting in a more compact structure with reduced free volume and lower WVT. The stronger intermolecular interactions between the polymer chains upon incorporation of PVA might have made the starch-PVA films more tortuous for water molecules to permeate, thereby reducing water vapor transmission. [26,28,37].

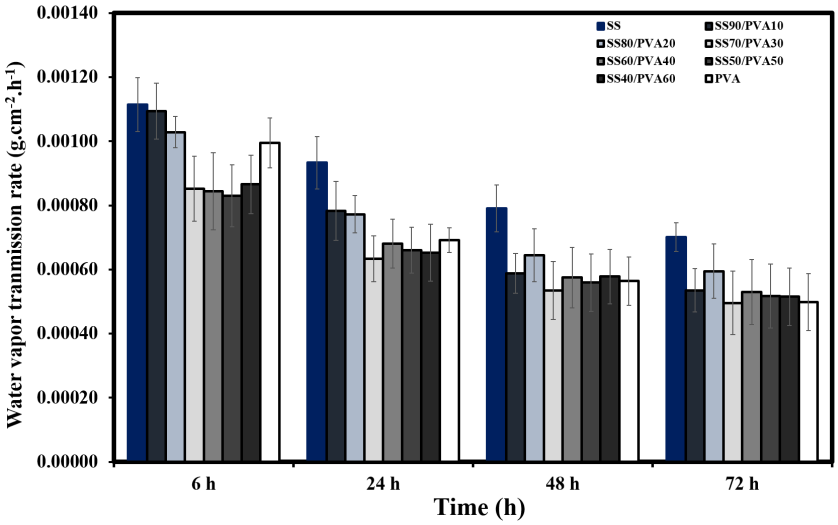


Figure 3 Water vapor transmission rate of SS, PVA, and SS/PVA biopolymer films with varying blending ratios measured after 6, 24, 48, and 72 h.

Water solubility

Water solubility (WS) of SS/PVA films indicates the amount of soluble matter after immersion in water 24 h as shown in **Figure 4**. High WS values of the film samples were expected because all constituents, including starch, PVA, and glycerol, are hydrophilic in nature. These results are consistent with previous studies [37].

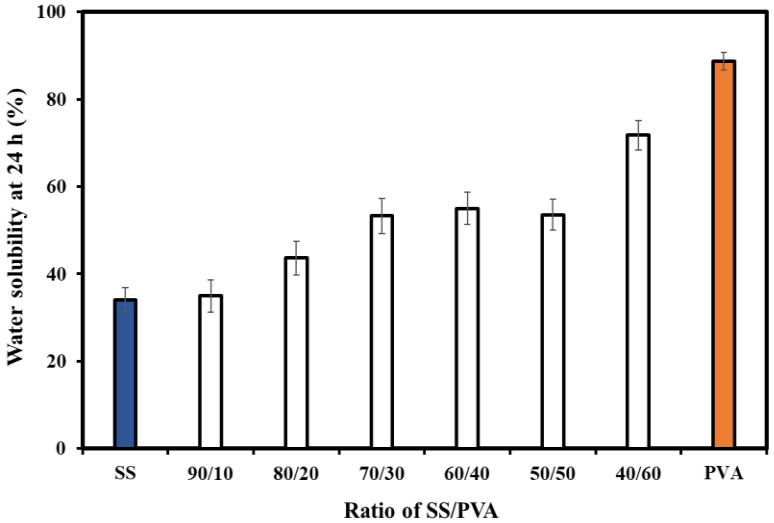


Figure 4 Water solubility after 24 h immersion of SS, PVA, and SS/PVA biopolymer films with varying blending ratios.

Pure PVA film was almost completely soluble in water, showing about 88% solubility in water within 24 h. Nevertheless, pure starch exhibited significantly lower WS (35.3%) than pure PVA film. This can be attributed to the inherently higher water affinity of PVA and its greater chain mobility in aqueous environments. The abundance of hydroxyl groups along the PVA backbone facilitates extensive hydrogen bonding with water molecules, promoting swelling and ultimately enhancing film solubility [25,27,37]. At low PVA incorporation (SS90/PVA10), WS remains comparable to SS film, suggesting limited disruption of the starch network. However, a marked increase is observed from 80/20 onward, indicating enhanced water accessibility and partial weakening of intermolecular interactions. Notably, the WS trend is not strictly linear, as evidenced by the slight decrease at SS50/PVA50 compared to SS60/PVA40. This suggests that improved intermolecular hydrogen bonding between starch and PVA promotes a more compact structure, temporarily

limiting solubility. In contrast, at higher PVA content (40/60), the water solubility (WS) markedly increased to 71.80%, due to the highly hydrophilic nature of PVA and its sensitivity to moisture, which facilitate water penetration and polymer dissolution. These results are consistent with previous studies [37].

Water contact angle

The water contact angle (WCA) of the SS/PVA films reflected their surface wettability and hydrophilicity as presented in **Figure 5**. All film samples exhibited WCA values below 90°, indicating their hydrophilic nature, which was consistent with the water solubility results. The neat SS film exhibited the highest contact angle (89.3°), indicating relatively low surface hydrophilicity as compare to SS/PVA and PVA films. This behavior can be attributed to the semi crystalline structure of starch and the limited availability of free hydroxyl groups at the film surface. In contrast, pure PVA exhibited the lowest contact angle (43.8°) of water, confirming its highly hydrophilic nature due to the abundance of hydroxyl (-OH) groups that readily interact with water molecules. This is in agreement with the previous result [22,37,38)]. The SS/PVA blend films displayed contact angle values in the range of approximately 50° - 70°, demonstrating that the incorporation of PVA enhances surface hydrophilicity compared to SS film. At low PVA content (SS90/PVA10 and SS80/PVA20), a pronounced slightly decrease in contact angle was observed, indicating that even small amount of PVA strongly influence surface wettability. At SS/PVA mixing ratio of 70/30, 60/40, and 50/50, the contact angle increased slightly but not significantly, indicating strong intermolecular interactions, particularly hydrogen bonding between SS and PVA, which may reduce the number of free hydroxyl groups present on the film surface. At higher PVA content (SS40/PVA60), the contact angle of water significantly decreased and approached that of pure PVA film, implying the dominance of PVA at the film surface. Patil *et al*. [37], reported that the water contact angle (WCA) of polymeric surfaces decreases with increasing amounts of polar functional groups, such as C=O and -OH groups. These groups are capable of forming hydrogen bonds with water molecules, thereby enhancing surface wettability. FTIR analysis in the present study revealed that blending PVA with starch increased the intensity of hydrophilic functional groups, particularly C=O and -OH groups, which likely contributed to the reduction in WCA observed in the blend film samples [37]. SEM observations also revealed that the SS/PVA blend films exhibited a more homogeneous and compact morphology compared to neat SS film, indicating improved compatibility between the polymer phases.

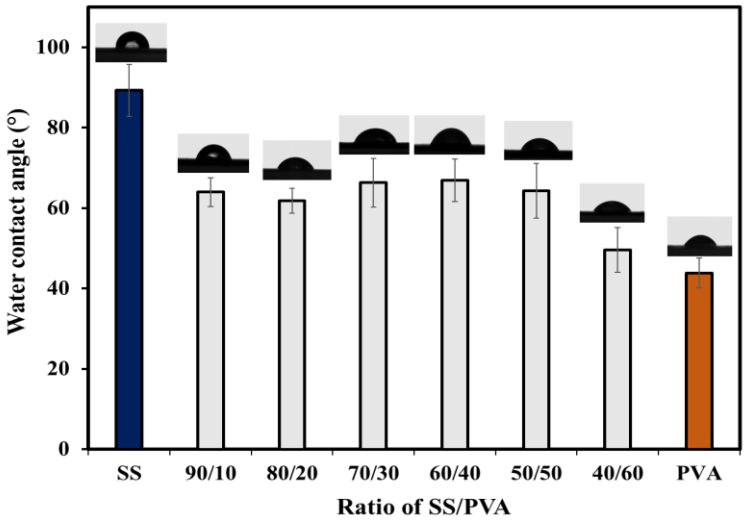


Figure 5 Water contact angle measured on the surface of SS, PVA, and SS/PVA biopolymer films with varying blending ratios.

Mechanical properties of SS/PVA biopolymer films

The tensile properties of SS/PVA films were evaluated by calculating stress and strain to determine tensile strength, elongation at break, and modulus as illustrated in **Figure 6**.

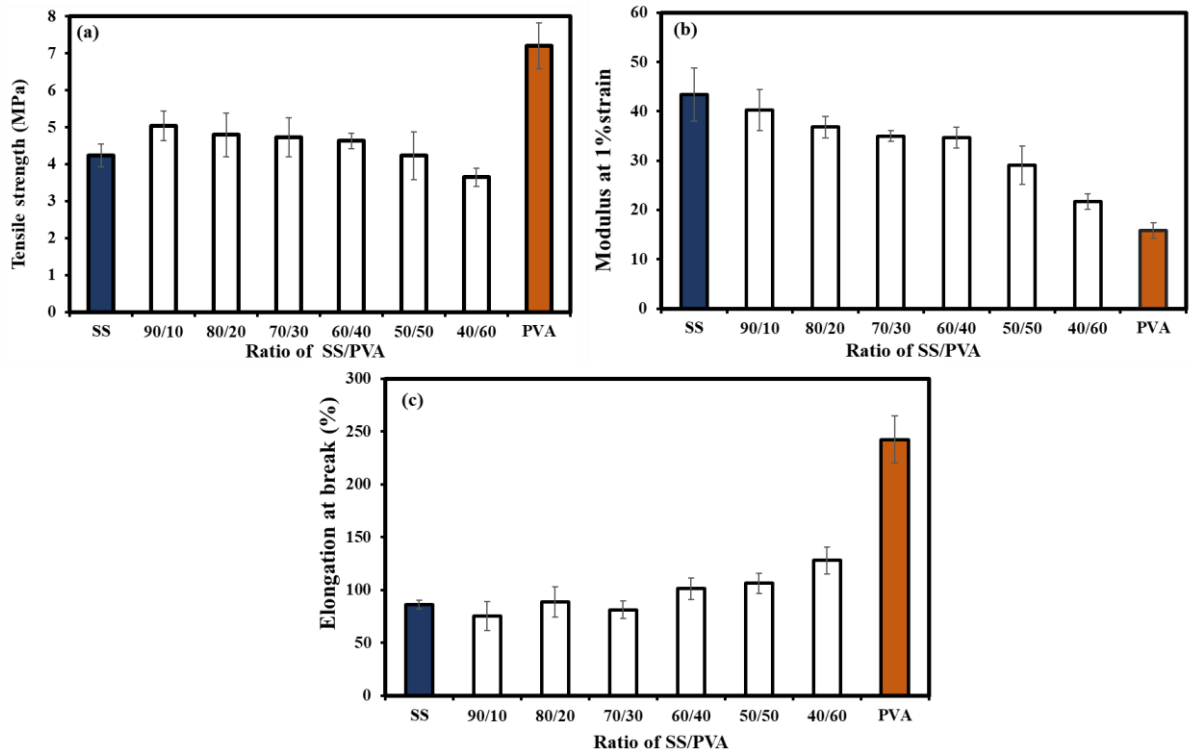


Figure 6 Tensile strength (a), modulus at 1% strain (b), and elongation at break (c) of SS, PVA, and SS/PVA biopolymer films with varying blending ratios.

Figure 6(a) presents the tensile strength (TS) of the SS/PVA blend films. The pure SS film exhibited a relatively low TS value of 4.23 MPa, which is characteristic of starch-based films due to their inherently brittle nature and limited intermolecular interaction. With increasing PVA content, the TS of the SS/PVA blend films (SS90/PVA10 to SS60/PVA40) gradually increased compared with the pure SS film. It can be attributed to enhance some intermolecular interaction between SS and PVA, particularly, hydrogen bonding between the hydroxyl groups of both polymers. At the SS50/PVA50 ratio, the TS value slightly decreased to 4.23 MPa, suggesting the onset of a balance between effect of intermolecular interaction and the plasticizing effect associated with increased PVA content. A more pronounced reduction in TS was observed for the SS40/PVA60 film (3.65 MPa), which may be related to excessive PVA incorporation, resulting in reduced intermolecular cohesion within the blend matrix and increased polymer chain mobility. In contrast, the pure PVA film exhibited the highest TS value (7.20 MPa), reflecting its superior film-forming capability and stronger intermolecular interactions compared with starch-based films [37,39].

Figure 6(b) illustrates the modulus at 1% strain of the SS/PVA blend films as a function of blend composition. The sago starch (SS) film exhibited the highest modulus value (≈46 MPa), resulting the rigid nature of the starch and the extensive hydrogen-bonding interaction within the polysaccharide network, which provide high resistance to elastic deformation. As the PVA content increased, the modulus gradually decreased, indicating progressive softening of the film structure and reduced stiffness of the blend films. The SS/PVA films with ratio of 90/10, 80/20, and 70/30 slightly decreased modulus values. This is due to starch remained the dominant load-bearing component, and PVA primarily functioned as a flexible or plasticizing

phase within the blend [28,39]. However, when the PVA content exceeded 50% (SS50/PVA50 and SS40/PVA60), a more pronounced reduction in modulus was observed, with the pure PVA film exhibiting the lowest modulus value (15.8 MPa). This substantial decrease indicates a transition from a starch-dominated rigid network to a PVA-dominated flexible matrix.

The elongation at break (EB) elucidates the mechanical behavior of the SS/PVA films as illustrated in **Figure 6(c)**. The pure SS film showed an elongation of approximately 85%, reflecting its rigid and brittle matrix, which restricts molecular mobility and limits deformation under tensile stress. The SS/PVA ratio of 90/10, 80/20, and 70/30 yielded EB values in the range of 70% - 90%, indicating only marginal enhancement in ductility, as the starch network remained mechanically dominant. SS/PVA films with ratio of 60/40, 50/50, and 40/60 exhibited sightly increasing of EB value. The PVA film showed the highest elongation at break, approaching 250%, due to its inherently flexible, ductile and energy absorbing polymeric structure [28,36,37]. As the PVA fraction increases, the SS/PVA blend network becomes progressively softer and more extensible. In the absence of starch, pure PVA exhibited maximum ductility and superior resistance to fracture under tensile loading.

Chemical structure, crystal structure and morphology of SS/PVA biopolymer films

UV-Visible absorption of SS/PVA biopolymer films

UV-visible spectroscopy is widely used for the analysis of chromophore groups of atoms characterized by strongly absorbing electronic transitions. The UV-visible absorption spectra of SS, PVA and SS/PVA films at various ratios clearly demonstrated the strong dependence of optical properties on polymer composition and intermolecular interaction as shown in **Figure 7**.

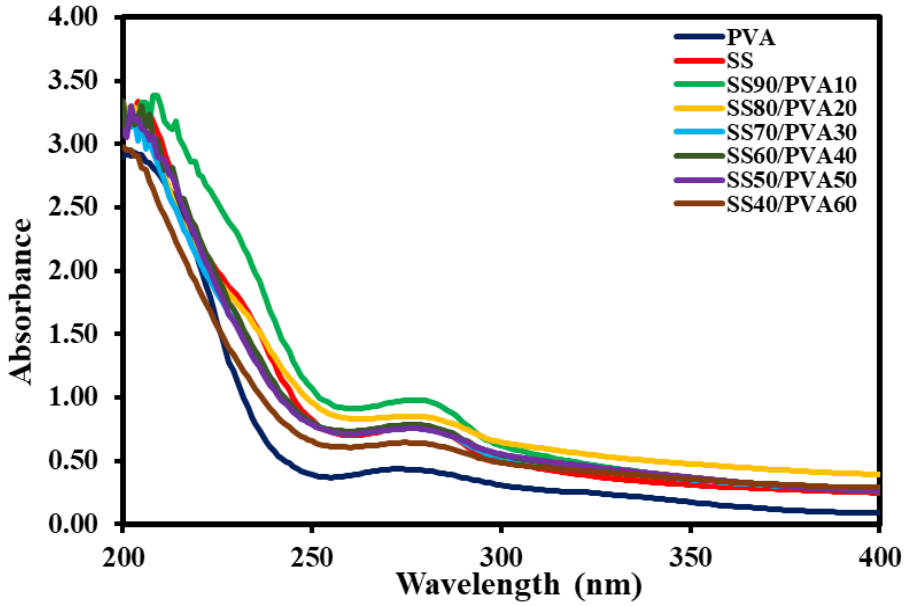


Figure 7 UV-visible spectra of SS, PVA, and SS/PVA biopolymer films with varying blending ratios recorded over the wavelength range of 200 - 400 nm.

The results revealed pronounced absorption in the ultraviolet (UV) region, with maximum absorbance occurring within the 200 - 240 nm range and a characteristic shoulder peak at approximately 250 - 300 nm. The absorption in the 200 - 240 nm region is attributed to electronic transitions in oxygen-containing functional groups, specifically the non-bonding electron transitions ($n \rightarrow \sigma^*$ and $n \rightarrow \pi^*$) of hydroxyl (-OH) groups present in both the starch and PVA chains [40,42]. An increase in starch content led to higher absorbance, which is ascribed to the abundance of hydroxyl groups and the semi-crystalline granular structure of starch. This structural characteristic enhances both intrinsic UV absorption and light scattering within the polymer

matrix. Similar trends have been reported for starch-based films, where the presence of crystalline domains and hydrogen bond rich networks improves UV shielding efficiency but reduces overall optical clarity. The pure PVA film exhibited a maximum absorbance at approximately 200 nm, corresponding to electronic transitions, along with a shoulder around 210 nm attributed to transitions from residual carbonyl (C=O) functional groups. Upon blending starch with PVA, the absorption maximum underwent a bathochromic (red) shift toward longer wavelengths, accompanied by a hyperchromic effect [40,42]. In the visible region (300 - 500 nm), all films displayed low absorbance, indicating good transparency. Films with higher PVA content exhibited further reduction in light scattering. Therefore, the SS/PVA ratio plays a critical role in determining the balance between UV shielding performance and optical transparency.

Fourier transform infrared spectroscopy

The FTIR spectra of SS, PVA, and their blend films confirm the presence of characteristic functional groups and intermolecular interactions, as shown in **Figure 8**. Both SS and PVA films exhibited a broad absorption band at 3,140 - 3,390 cm^{-1}, corresponding to O-H stretching vibration of hydroxyl groups in polysaccharide and PVA chains, indicating extensive intra- and intermolecular hydrogen bonding within the polymer matrix. The absorption band at approximately 2,925 cm^{-1} was attributed to C-H stretching vibrations of aliphatic -CH and -CH_2 groups. For PVA, the peak at 845 cm^{-1} was assigned to symmetric C-C stretching, while the bands at 927 and 1,145 cm^{-1} corresponded to C-H bending and C-O-C stretching vibrations, respectively. The strong band at 1,242 cm^{-1} was attributed to C-O-H stretching, whereas the peaks at 1,033, 1,041, and 1,109 cm^{-1} were associated with C-O bending vibrations. In addition, the peaks at 1,371 and 1,427 cm^{-1} were assigned to CH_3 and -CH_2- bending vibrations. The absorption bands at 1,637 and 1,732 cm^{-1} corresponded to O-H bending of absorbed water and C=O stretching vibrations, respectively, which may be associated with residual acetate groups [22,41,43]. For SS/PVA blend films with high starch content (SS90/PVA10 and SS80/PVA20), the FTIR spectra were mainly dominated by starch-related features. The broad O-H stretching band at 3,140 - 3,390 cm^{-1} appeared intense and broad, indicating strong hydrogen bonding among polysaccharide chains. The characteristic C-O stretching band at 1,242 cm^{-1} was clearly observed, while the C=O stretching band near 1,732 cm^{-1} appeared only as a weak shoulder due to the low PVA content. As the PVA content increased (SS70/PVA30 and SS60/PVA40), noticeable changes occurred in the O-H stretching region, including increased intensity and a slight band shift, suggesting enhanced hydrogen bonding interaction between SS and PVA hydroxyl groups. The intensity of the band around 1,732 cm^{-1} also gradually increased, reflecting the greater contribution of residual acetate groups from PVA. In addition, subtle changes in the 1,242 cm^{-1} region indicate overlapping C-O stretching vibrations from both polymers, suggesting improved molecular compatibility. At higher PVA content (SS50/PVA50 and SS40/PVA60), the FTIR spectra became more characteristic of PVA. The O-H stretching band appeared smoother and slightly less intense than in starch-rich films, resulting rearrangement of hydrogen bonding dominated by PVA-PVA and PVA-SS interactions. The C=O stretching band at 1,732 cm^{-1} became more pronounced, confirming the increasing influence of PVA within the blend matrix [36].

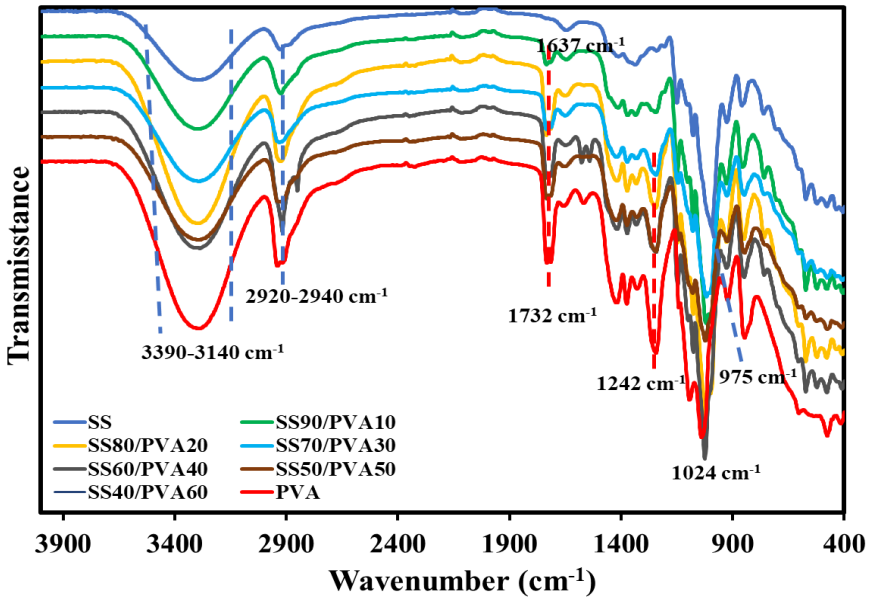


Figure 8 Fourier-transform infrared (FTIR) spectra of SS, PVA, and SS/PVA biopolymer films with varying blending ratios, recorded in the wavenumber of 400 - 4,000 cm^{-1}.

X-Ray diffraction analysis

X-ray diffraction (XRD) patterns of SS, PVA, and SS/PVA films are presented in **Figure 9**. The glycerol-plasticized sago starch film exhibited characteristic diffraction peaks at 2θ = 17.4°, 19.9°, and 22.8°, corresponding to a combination of A-type crystalline structure and V-hydrate (V_h) crystalline structure [32]. The peaks at 17.2° and 20.0° are associated with the interplanar spacing of the starch molecular arrangement, while the relatively sharp peak at 2θ = 22.1° indicates a higher degree of molecular ordering within the starch matrix. In contrast, the XRD patterns of the PVA film displayed prominent crystalline diffraction peaks at 2θ = 19.4° and 23.2°, respectively [41]. These peaks can be implied the semicrystalline nature of PVA, which arises from intra- and intermolecular hydrogen bonding among PVA chains [40,41]. Upon blending with more PVA content, the characteristic starch and PVA diffraction peaks slightly shift with combine at 2θ = 19.4° and 22.8° and became broader, indicating increment of hydrogen bonding between starch and PVA chains. The calculated crystallinity values further supported these structural changes. Pure SS and PVA films exhibited crystallinity values of 21.63% and 23.50%, respectively, while the SS/PVA blends showed values of 23.90% (80/20), 20.67% (60/40) and 14.67% (40/60). The slight increase in crystallinity for SS80/PVA20 suggests that a small amount of PVA promoted molecular rearrangement and chain packing through hydrogen-bond interactions. However, further increasing the PVA content progressively reduced crystallinity, indicating that strong starch-PVA interactions disrupted crystal formation and increased the amorphous character of the films. This trend is consistent with the broadened diffraction peaks observed in the XRD patterns. This observation is consistent with the FTIR results, which suggest the formation of intermolecular hydrogen bonding between SS and PVA, leading to reduced starch-starch interaction and partial destruction of ordered domain [37]. Consequently, variations in the SS/PVA ratio significantly influenced the crystalline structure of the blend films. Furthermore, the reduction in crystallinity at higher PVA contents is consistent with the observed decrease in water contact angle and increase in water affinity, as the larger amorphous fraction facilitates water penetration and enhances the accessibility of hydrophilic hydroxyl groups on the film surface.

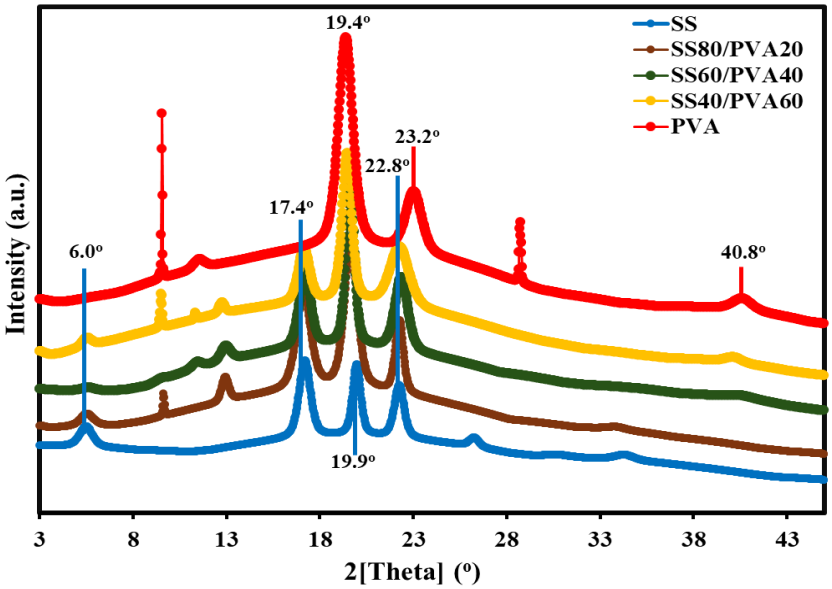


Figure 9 X-ray diffraction patterns of SS, PVA, and SS/PVA biopolymer films at blending ratios of 80/20, 60/40, and 40/60, recorded over a 2θ range of 3° - 45°.

DSC analysis of SS/PVA biopolymer films

DSC thermograms of SS, PVA, and SS/PVA films are shown in **Figure 10**. The DSC curves demonstrated that the thermal behavior of SS/PVA blend films strongly depended on blend composition, indicating changes in molecular interaction, crystallinity, and phase structure. Pure PVA film exhibited a sharp melting peak at approximately 215 °C, corresponding to the melting of crystalline PVA domain, confirming its semicrystalline structure [44]. This result is consistent with the XRD pattern, where pure PVA showed distinct crystalline diffraction peaks, and with the FTIR spectra revealing ordered intermolecular hydrogen bonding between PVA chains. In contrast, pure sago starch (SS) showed a broader endothermic peak around 210 °C, suggesting a predominantly amorphous structure with less organized molecular packing after gelatinization. This broad transition agrees with the XRD results showing reduced crystallinity of starch films and the FTIR spectra characterized by extensive hydrogen bonding within starch chains. For SS/PVA blend films, the thermal transition shifted depending on the blending ratio, implying intermolecular interaction and partial miscibility between SS and PVA. The SS90/PVA10, SS80/PVA20, SS70/PVA30, and SS60/PVA40 films showed melting transitions at higher temperatures (221 - 224 °C). This can be explained by stronger hydrogen-bonding interactions between SS and PVA [24,44]. This observation agrees with the FTIR results, which showed peak shifting and broadening in the O–H stretching region, indicating enhanced intermolecular interaction. In addition, XRD analysis revealed increased molecular ordering in SS/PVA films compared with pure SS film. Interestingly, the SS50/PVA50 film showed a peak at approximately 205 °C, demonstrating significant structural rearrangement and possible formation of a more compatible intermolecular network between SS and PVA. Meanwhile, the SS40/PVA60 film exhibited a broader peak at a lower temperature (198 °C), which may indicate reduced structural uniformity and increased chain mobility at high PVA content. This behavior may be associated with the phase heterogeneity observed in the SEM images and the higher hydrophilicity of PVA-rich films.

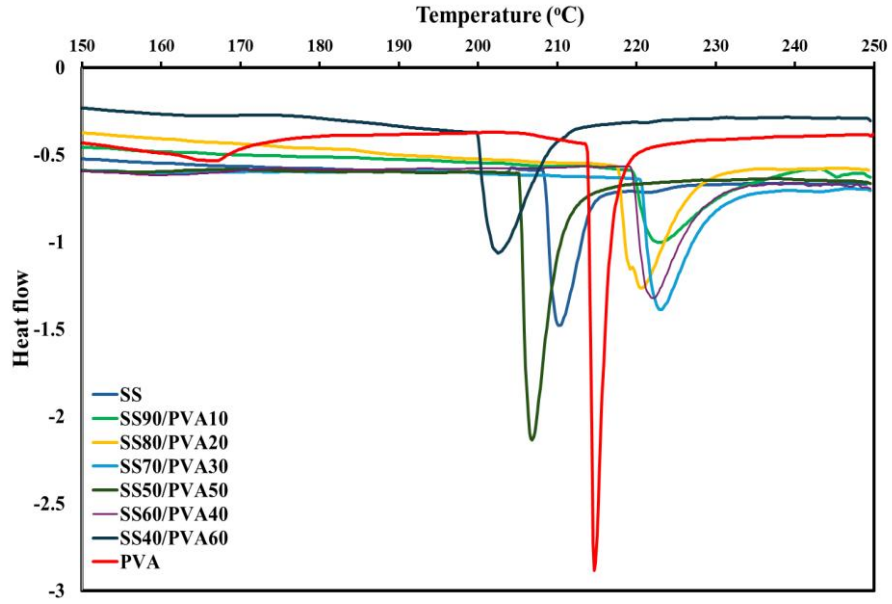


Figure 10 DSC thermograms of SS, PVA and SS/PVA biopolymer films with varying blending ratios recorded over the temperature range of 150 - 250 °C.

Morphology study of SS/PVA biopolymer films

The surface morphology of SS and SS/PVA films observed by using SEM is presented in **Figure 11**. The neat SS film exhibited a relatively smooth surface with the presence of small cracks, reflecting the inherent brittleness and limited mechanical strength of sago starch-based film. Similar microstructural features have been reported in previous studies on starch film [36,37,43]. Incorporation of PVA significantly altered the film morphology. The SS80/PVA20 film showed a smooth, homogeneous, and crack-free surface, indicating good dispersion of PVA and strong interfacial compatibility between SS and PVA at this composition. This morphological uniformity is consistent with earlier reports demonstrating that moderate PVA content enhances hydrogen bonding with starch, resulting in improved water resistance and reduced water vapor permeability [37,38]. In contrast, films with higher PVA content (SS50/PVA50 and SS40/PVA60) displayed pronounced surface roughness, wrinkle, microcrack, and small pores. As PVA content increases, starch polymer reversed to dispersed phase from continuous phase, depicting the miscibility of amorphous portion of starch with PVA. These results agree well with previous studies reporting an optimal starch-to-PVA ratio that maximizes intermolecular interactions while preventing phase separation [37].

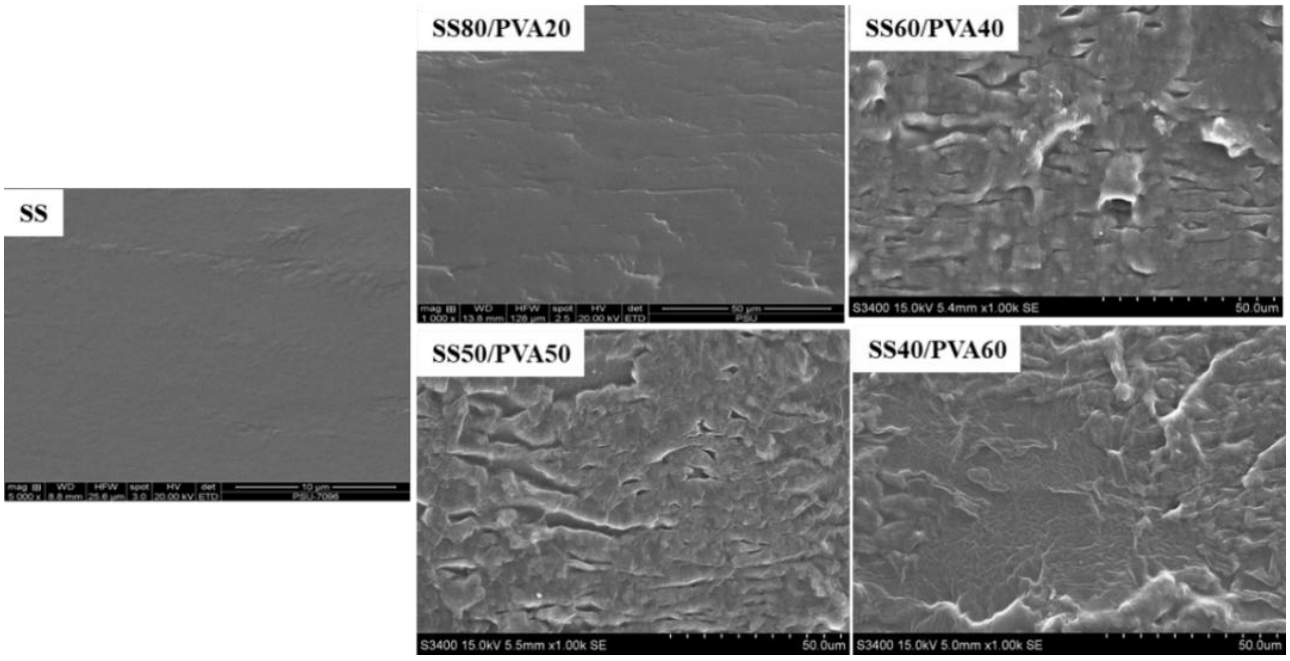


Figure 11 SEM micrographs of SS and SS/PVA biopolymer films with varying blending ratios at a magnification of 1.00kx.

Structure-properties relationship of SS/PVA biopolymer films

From the research results, the interaction within the film can be illustrated as shown in **Figure 12**.

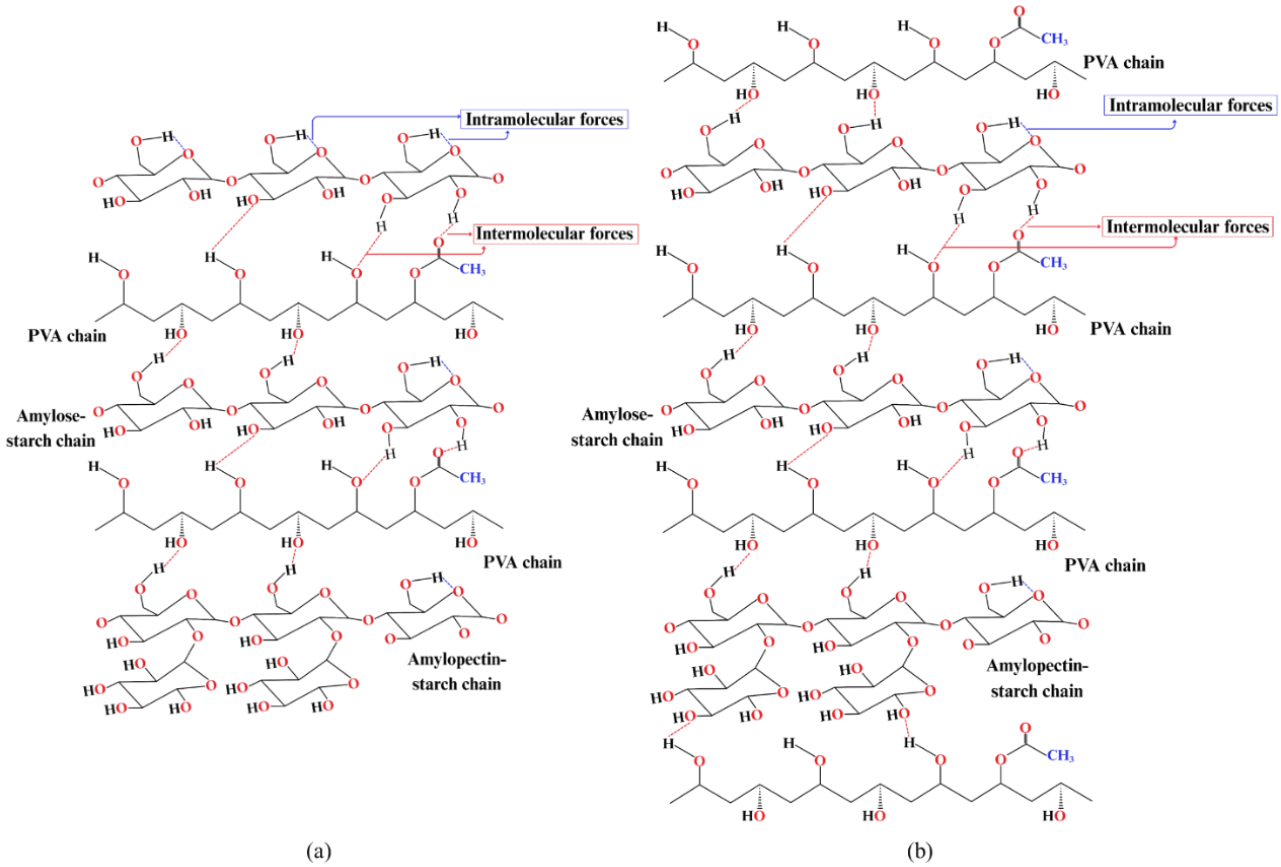


Figure 12 Schematic illustration of intermolecular interactions between SS and PVA in biopolymer films: (a) SS-rich composition and (b) PVA-rich composition.

For biopolymer films with a high starch ratio (e.g., SS/PVA ratios of 90/10, 80/20, and 70/30), the film structure is controlled by a gelatinized starch network containing a large number of hydroxyl (-OH) groups. This results in efficient hydrogen bonds, both between starch chains themselves (SS-SS) and between starch and polyvinyl alcohol (SS-PVA). When low to moderate amounts of PVA are added, it can be uniformly distributed within the starch matrix through interchain interaction, causing in a denser and more continuous film structure. This interaction enhances the mechanical properties and reduces the water vapor transmission of high starch ratio films. Furthermore, they display a higher water contact angle (WCA) which indicate superior surface wetting ability. This is because some hydroxyl groups participate in hydrogen bonding within the film structure, reducing the number of free hydroxyl groups on the surface. FTIR analysis confirms physicochemical interaction via hydrogen bonding, while XRD and DSC analysis reveal interaction affecting polymer chain arrangement, crystallinity, and movement. SEM provides morphological evidence of continuous and compatible film structure at the microscopic level. These findings show that films with a high SS content have a denser and stronger structure, as well as better water resistance, compared to films with a high PVA content.

Conclusions

Starch is a biodegradable and renewable polymer with strong potential for sustainable packaging applications. In this study, sago starch, which provides a favorable balance between film-forming ability, was blended with polyvinyl alcohol at different ratio to improve the physical, barrier, thermal, and structural properties of SS/PVA films. The results showed that PVA incorporation significantly affected film performance depending on blend composition. Increasing PVA content enhanced film flexibility and reduced water vapor transmission rate (WVTR), indicating improved barrier properties through stronger intermolecular interaction. However, higher PVA content increased film transparency and water solubility due to its hydrophilic nature and higher chain mobility. FTIR analysis confirmed hydrogen bonding interaction between SS and PVA, while XRD and DSC results revealed the increment of increased molecular arrangement and semicrystalline characteristic with increasing PVA content. SEM images revealed rougher and more heterogeneous morphologies at high PVA ratio. Considering the balance between structure–property relationships, the SS80/PVA20, SS70/PVA30, and SS60/PVA40 blend ratio exhibited the most promising overall performance for biodegradable packaging applications.

Acknowledgements

This work is supported by Pattani campus research fund, Prince of Songkla University, Pattani Campus (No. SAT6603014S) Pattani, Thailand.

Declaration of generative AI in scientific writing

The authors use of generative artificial intelligence tools, including Grammarly, ChatGPT by OpenAI, particularly for language editing and grammar improvement. The AI tools were not used to generate scientific content or interpret data. The authors take full responsibility for the content and conclusions of this research.

CRediT author statement

Pattamarat Rattanachuay: Methodology; Software; Visualization; Writing - Original draft preparation. **Sameela Cheming:** Methodology; Data curation; Formal analysis; Investigation **Lapporn Vayachuta:** Software; Visualization; Investigation; Writing - Reviewing and Editing. **Jareerat Ruamcharoen:** Conceptualization; Methodology; Validation; Supervision; Writing - Original draft preparation; Writing - Reviewing and Editing; Project administration.

References

[1] H Onyeaka, K Obileke, G Makaka and N Nwokolo. Current research and applications of starch-based biodegradable films for food packaging. *Polymers* 2022; **14(6)**, 1126.

[2] D Dutta and N Sit. A comprehensive review on types and properties of biopolymers as sustainable bio-based alternatives for packaging. *Food Biomacromolecules* 2024; **1(2)**, 58-87.

[3] SP Bangar and WS Whiteside. Nano-cellulose reinforced starch bio composite films - A review on green composites. *International Journal of Biological Macromolecules* 2021; **185**, 849-860.

[4] EE Sirbu, A Dinita, M Tănase, AI Portoacă, A Bondarev, CE Enascuta and C Calin. Influence of plasticizers concentration on thermal, mechanical, and physicochemical properties on starch films. *Processes* 2024; **12(9)**, 2021.

[5] K Miller, C Silcher, M Lindner and M Schmid. Effects of glycerol and sorbitol on optical, mechanical, and gas barrier properties of potato peel-based films. *Packaging Technology and Science* 2021; **34(1)**, 11-23.

[6] L Arroyo-Esquivela, VM Jiměnezc, F Vásquezd and P Esquivel. Plasticizers improved flexibility, homogeneity, and color stability in pitahaya (*Hylocereus* sp.) peel-based biopolymer films aimed at food packaging. *Industrial Crops and Products* 2025; **227**, 120757.

[7] MA Otache, RU Duru, O Achugasim and OJ Abayeh. Advances in the modification of starch via esterification for enhanced properties. *Journal of Polymers and the Environment* 2021; **29**, 1365-1379.

[8] SP Bangar, KV Sunooj, M Navaf, Y Phimolsiripol and WS Whiteside. Recent advancements in cross-linked starches for food applications- a review. *International Journal of Food Properties* 2024; **27(1)**, 411-430.

[9] FM Fakhouri, SM Martelli, T Caon, JI Velasco and LHI Mei. Edible films and coatings based on starch/gelatin: Film properties and effect of coatings on quality of refrigerated Red Crimson grapes. *Postharvest Biology and Technology* 2015; **109**, 57-64.

[10] PA Pawase, AM Pathare, O Bashir, F Saleem, E Shrama, S Mudgal and M Ahmad. Physical, chemical, and nano-enabled modifications of starch for sustainable food packaging films: Recent trends, challenges, and prospects. *Carbohydrate Polymer Technologies and Applications* 2025; **11**, 100986.

[11] F Zhu. Starch based films and coatings for food packaging: Interactions with phenolic compounds. *Food Research International* 2025; **204**, 115758.

[12] C Campanale, S Galafassi, FD Pippo, I Pojar, C Massarelli and VF Uricchio. A critical review of biodegradable plastic mulch films in agriculture: Definitions, scientific background and potential impacts. *Trends in Analytical Chemistry* 2024; **170**, 117391.

[13] S Wannaphatchaiyong, J Suksaeree, R Waiprib, A Kaewpuang, W Saelee and W Pichayakorn. Gelatin/gelatinized sago starch biomembranes as a drug delivery system using rubber latex as plasticizer. *Journal of Polymers and the Environment* 2019; **27**, 2380-2394.

[14] EF Tethool, S Raharjo, Y Pranoto and S Supriyadi. Investigation of pregelatinized sago starch-decanoic acid complex by ultrasonication and its potential to stabilize oil-in-water emulsion. *Trends in Sciences* 2025; **22(3)**, 9241.

[15] FB Ahmad, PA Williams, JL Doublier, S Durand and A Buleon. Physico-chemical characterisation of sago starch. *Carbohydrate Polymers* 1999; **38(4)**, 361-370.

[16] SN David Chua, EP Kho, SF Lim and MH Hussain. Sago palm (*Metroxylon sagu*) starch yield, influencing factors and estimation from morphological traits. *Advances in Materials and Processing Technologies* 2022; **8(2)**, 1845-1866.

[17] C Du, F Jiang, W Jiang, W Ge and SK Du. Physicochemical and structural properties of sago starch. *International Journal of Biological Macromolecules* 2020; **164**, 1785-1793.

[18] A Mittal, S Garg, A Premi and AS Giri. Synthesis of polyvinyl alcohol/modified starch-based biodegradable nanocomposite films reinforced with starch nanocrystals for packaging applications. *Polymers and Polymer Composites* 2021; **29(5)**, 405-416.

[19] HC Oyeoka, CM Ewulonu, IC Nwuzor, CM Obele and JT Nwabanne. Packaging and degradability properties of polyvinyl alcohol/gelatin nanocomposite films filled water hyacinth cellulose nanocrystals. *Journal of Bioresources and Bioproducts* 2021; **6(2)**, 168-185.

[20] S Sharma, K Nakano, S Kumar and V Katiyar. Edible packaging to prolong postharvest shelf-life of fruits and vegetables: A review. *Food Chemistry Advances* 2024; **4**, 100711.

[21] TA Nguyen and VH Nguyen. High-performance flame-retardant PVA/nanoclay/MWCNTs composite films: Fabrication, multifunctional properties, and advanced characterization. *Trends in Sciences* 2025; **22(9)**, 10219.

[22] R Hussain, SA Batool, A Aizaz, M Abbas and MAU Rehman. Biodegradable packaging based on poly (vinyl alcohol) and carboxymethyl cellulose films incorporated with ascorbic Acid for food packaging application. *ACS Omega* 2023; **8(45)**, 42301-42310.

[23] N Park, MA Friest and L Liu. Enhancing the properties of polyvinyl alcohol films by blending with corn stover-derived cellulose nanocrystals and beeswax. *Polymers* 2023; **15(21)**, 4321.

[24] WA Rahman, LT Sin, AR Rahmat and AA Samad. Thermal behaviour and interactions of cassava starch filled with glycerol plasticized polyvinyl alcohol blends. *Carbohydrate Polymers* 2010; **81(4)**, 805-810.

[25] R Yahia, ME Owda, RE Abou-Zeid, F Abdelhai, HY El-Gamil, AM Abdo and AA Ali. Biodegradable, UV absorber and thermal stable bioplastic films from waxy corn starch/polyvinyl alcohol blends. *Biomass Conversion and Biorefinery* 2024; **14**, 27989-28006.

[26] MMR Khan and MMH Rumon. Synthesis of PVA-based hydrogels for biomedical applications: Recent trends and advances. *Gels* 2025; **11(2)**, 88.

[27] JM Castro, MG Montalbán, N Martínez-Pěrez, D Domene-L´opez, JM P´erez, FM Arrabal-Campos, I Fernández, I Martín-Gullón and JC García-Quesada. Thermoplastic starch/polyvinyl alcohol blends modification by citric acid–glycerol polyesters. *International Journal of Biological Macromolecules* 2023; **244**, 125478.

[28] BA Omoike, FE Okieimen, C Imoisi and MA Abubakar. Characterization and evaluation of properties of cassava starch/poly (Vinyl alcohol) films for food and pharmaceutical packaging applications. *Singapore Journal of Scientific Research* 2024; **14(1)**, 34-42.

[29] K Lu, C Post, J Hu, D Maniar, R Folkersma, VSD Voet and K Loos. Structure and properties of biodegradable self-healing starch/PVA/chitosan hydrogels. *Polymer* 2025; **336**, 128864.

[30] AOAC. *Official methods of analysis*. 17th ed. The Association of Official Analytical Chemists, Gaithersburg, 2000.

[31] ASTM International. *ASTM E96/E96M-24: Standard test methods for water vapor transmission of materials*. ASTM International, Pennsylvania, 2024.

[32] J Ruamcharoen, R Munlee and P Ruamcharoen. Eco-friendly bio-based composites of cassava starch and natural rubber compatibilized with nanoclays. *Polymer Composites* 2023; **44(2)**, 1071-1082.

[33] ASTM International. *ASTM D882-12 Standard test method for tensile properties of thin plastic sheeting*. ASTM International, Pennsylvania, 2014.

[34] DNA Wahab, MBM Siddique, JJ Chew, HT Su, N Khairuddin, DS Khaerudini, MS Hossain and J Sunarso. Characterization of starch biofilm reinforced with cellulose microfibers isolated from Musa *Saba'* midrib residue and its application as an active packaging film. *Journal Applied Polymer Science* 2023; **140(48)**, e54720.

[35] ZZ Tryznowska and A Kałuza. The influence of starch origin on the properties of starch films: Packaging performance. *Materials* 2021; **14(5)**, 1146.

[36] C Shanbhag, R Shenoy, P Shetty, M Srinivasulu and R Nayak. Formulation and characterization of starch-based novel biodegradable edible films for food packaging. *Journal of Food Science and Technology* 2023; **60(11)**, 2858-2867.

[37] S Patil, AK Bharimalla, A Mahapatra, J Dhakane-Lad, A Arputharaj, M Kumar, ASM Raja and N Kambli. Effect of polymer blending on mechanical and barrier properties of starch-polyvinyl alcohol based biodegradable composite films. *Food Bioscience* 2021; **44(A)**, 101352.

[38] ZW Abdullah and Y Dong. Biodegradable and water resistant poly (Vinyl alcohol) (PVA)/starch (ST)/glycerol (GL)/halloysite nanotube (HNT) nanocomposite films for sustainable food packaging. *Frontiers in Materials* 2019. https://doi.org/10.3389/fmats.2019.00058

[39] MK Chan and TH Tang. The properties of starch/cellulose/polyvinyl alcohol composite as

hydrodegradable film. *Polymers and Polymer Composites* 2022; **30**, 1-8.

[40] S Masood, L Gulnar, AD Chandio, H Arshad, W Rehman and A Atique. Preparation and optical characterization of poly (Vinyl alcohol) and starch (native and modified) blend films. *Journal of Polymer Research* 2022; **29**, 528.

[41] SN Kareem, MH Suhail and OG Abdullah. Effect of salt content and operating temperature on the nitrogen dioxide gas sensing performance of sodium-ion conducting solid polymer electrolyte. *Trends in Sciences* 2023; **20(10)**, 5890.

[42] HN Wei, XY Liu, CC Wang, R Feng and B Zhang. Characteristics of corn starch/polyvinyl alcohol composite film with improved flexibility and UV shielding ability by novel approach combining chemical cross-linking and physical blending. *Food Chemistry* 2024; **456**, 140051.

[43] Guimarães, VR Botaro, KM Novack, FG Teixeira and GHD Tonoli. High moisture strength of cassava starch/polyvinyl alcohol-compatible blends for the packaging and agricultural sectors. *Journal of Polymer Research* 2015; **22**, 192.

[44] OW Guirguis and MTH Moselhey. Thermal and structural studies of poly (Vinyl alcohol) and hydroxypropyl cellulose blends. *Natural Science* 2012; **4(1)**, 57-67.